Hartree-Fock-Roothaan calculations for many-electron atoms and ions in neutron-star magnetic fields

Dirk Engel and Günter Wunner
Institut für Theoretische Physik 1, Universität Stuttgart, D-70550 Stuttgart, Germany
(Dated: August 4, 2008)

The quantitative analysis of the electromagnetic spectra of isolated neutron stars by means of model atmosphere calculations requires extensive data sets of atomic energy values and transition probabilities in intense magnetic fields. We present a new method for the fast computation of wave functions, energies, and oscillator strengths of medium-Z atoms and ions at neutron star magnetic field strengths $B \gtrsim 10^7$ T which strikes a balance between numerical accuracy and computing times. We use a Hartree-Fock ansatz in which each single-electron orbital is expanded in terms of Landau states with one longitudinal expansion function, and each Landau level contributes with a different weight to the orbital. Both the longitudinal expansion functions and the Landau weights are determined in a doubly self-consistent way. Hartree-Fock equations are solved by decomposing the z axis in finite elements and expanding the longitudinal wave functions in terms of sixth-order B-splines. The contributions of the eight lowest Landau levels are taken into account. The procedure can be efficiently parallelized. Results are presented for the ground states and different excited states of atoms and ions for nuclear charges $Z = 2, \ldots, 26$ and $N = 2, \ldots, 26$ electrons, and for oscillator strengths. Wherever possible, a comparison with the results of previous calculations is made.

PACS numbers: 31.15.xr, 31.15.ag, 32.60.+i, 71.10.-w

I. INTRODUCTION

The observation of the thermal emission spectra of isolated neutron stars with temperatures of a few 10^5 K, made possible by the launch of two X-ray satellites at the end of the nineties, the Chandra X-Ray Observatory by NASA and the XMM-Newton Observatory by ESA, and the subsequent discovery of features in the X-ray spectra of the neutron star 1E 1207 [1, 2] and three other isolated neutron stars [3–5] has given new impetus to studies of atoms and ions with medium-Z nuclear charge numbers in strong magnetic fields [6–8]. The reason is that the observed features could be due to atomic transitions in elements that are fusion products of the progenitor star, and thus constituents of the thin atmospheres that cover the neutron star surfaces. The elemental compositions of the atmospheres are presently not yet well known, and any element between H and Fe is feasible [7]. However, to calculate synthetic spectra for model atmospheres, and thus to be in a position to draw reliable conclusions from observed spectra to the elemental composition of the atmospheres and the distribution of elements on different ionization stages, accurate atomic data for these elements at very strong magnetic fields are indispensible.

Atomic structure is entirely rearranged in neutron star magnetic fields since the effects of the magnetic field become of the same order of or even larger than those of the Coulomb binding. In particular, the familiar shell structure of atoms is completely lost. While the atomic properties of hydrogen and partly also helium at such field strengths have been elucidated in great detail in the literature over the past 25 years, for elements with nuclear charge numbers $Z > 2$ atomic data with the accuracy required for the calculation of synthetic spectra are available to a much lesser extent (references to the methods used and results obtained can be found, e.g,. in [9]). The challenge is to develop methods which allow one to calculate the energies (ground states and excited states) and oscillator strengths of medium-heavy atoms and ions up to iron ($Z = 26$) fast, routinely, and with sufficient accuracy.

In a parallel approach [9] we have tackled the problem from the side of diffusion quantum Monte Carlo (DQMC) simulations. The method has the advantage that ground state energies can be calculated practically free of approximations. The price to be paid, however, is computing times, even with parallelization, of up to a few hours for the heavy elements. Moreover, so far the DQMC method has been restricted to ground states.

In this paper we will pursue a different avenue, namely a Hartree-Fock approach. Our starting point is the expansion of the single-electron orbitals from which the Slater determinants are constructed in the complete basis of Landau states (Landau quantum numbers $n \geq 0$), with z-dependent expansion functions for each Landau state (the magnetic field is assumed to point in the z-direction). The self-consistent calculation of all longitudinal expansion functions would lead to a computational effort which is comparable to that of the DQMC method, and thus would entail no progress as far as the routine production of atomic data with sufficient accuracy is concerned. The feature of our approach then is to introduce the approximation that the expansion functions for each definite orbital are identical, for all Landau levels, while each Landau level contributes with a different weight to the expansion of the single-electron orbital. This approximation is based on the observation made in calculations for the hydrogen atom in a strong magnetic field [10] that the z-dependent expansion functions belonging to excited Landau levels essentially follow the character of

the expansion function of the lowest Landau level.

Both the z-dependent expansion functions of the individual orbitals and their Landau weights are determined self-consistently. Since the energy terms depend on all longitudinal wave functions and all Landau weights, in each iteration step the expansion functions determine the weights, and the weights the expansion functions. As usual the iteration is continued until convergence is achieved. The expansion of orbitals in terms of a sum of given orbitals with unknown weight coefficients is known in quantum chemistry as a Hartee-Fock-Roothaan ansatz (cf. [11, 12]). Since we describe the longitudinal wave functions by B-spline interpolation on finite elements, we adopt for our new method the name Hartree-Fock-Finite-Element-Roothaan (HFFER) method.

Our method contains as a special case (inclusion of the lowest Landau level $n = 0$ only) the Hartree-Fock ansatz in "adiabatic approximation" [13] used in the literature before [14–17]. Our method also is the self-consistent extension of the MCPH^3 (multi-configurational perturbative hybrid Hartree-Hartree-Fock) method introduced by Mori and Hailey [6]. In that method the exchange energy is taken into account only in first-order perturbation theory, in a basis of Hartree states obtained in adiabatic approximation, and the back-reaction of the excited Landau states, whose weights are taken into account perturbatively, on the effective interaction potentials is neglected. By contrast, our method includes both exchange terms and Landau weights in a fully self-consistent way.

In Sec. II we present in detail the constituent stages of our Hartree-Fock-Finite-Element-Roothaan method. Results are discussed in Sec. III and conclusions drawn in Sec. IV.

II. THE HFFER METHOD

A. Variational principle

Measuring energies in units of the Rydberg energy $E_{\rm Ryd}$, lengths in units of the Bohr radius a_0, and the magnetic field strength in units of $B_0 = 2\alpha^2 m_{\rm e}^2 c^2/(e\hbar) \approx 4.701 \times 10^5$ T, one can write the nonrelativistic Hamiltonian of an atom or ion with nuclear charge Z and N electrons in a uniform magnetic field as

$$\hat{H} = \sum_{i=1}^{N} \Bigg[- \Delta_{z_i,\rho_i,\varphi_i} - 2{\rm i}\beta \frac{\partial}{\partial\varphi_i} + \beta^2\rho_i^2 + 2\beta\hat{\sigma}_{z_i} - \frac{2Z}{|\mathbf{r}_i|}\Bigg] + \sum_{\substack{i,j=1\\ i<j}}^{N} \frac{2}{|\mathbf{r}_i - \mathbf{r}_j|}\,. \quad (1)$$

In (1), $\beta = B/B_0$ is the dimensionless magnetic field parameter. Since at neutron star magnetic field strengths the single-particle Coulomb excitation energies are much smaller than the spin flip energies, i.e, the cyclotron energy $\hbar\omega_B (\geq 1$ keV for $B \geq 10^7$ T), we can restrict ourselves to electrons in spin-down states and ignore the spin quantum number in what follows.

The reference magnetic field B_0 is characteristic of the switch-over from Coulomb to magnetic field dominance in the hydrogen atom. For nuclear charges $Z > 1$ the switch-over is shifted to the higher magnetic field strengths $B_Z = Z^2 B_0 \approx Z^2\ 4.701 \times 10^5$ T. The physical meaning is that for $B = B_Z$ the Larmor radius $a_{\rm L} = \sqrt{2\hbar/eB}$ becomes equal to the effective Bohr radius $a_Z = a_0/Z^2$, and the cyclotron energy is four times the effective Rydberg energy $E_Z = Z^2 E_{\rm Ryd}$.

The most general Hartree-Fock ansatz is to construct a Slater determinant

$$\Psi(\mathbf{r}_1, \ldots, \mathbf{r}_N) = \frac{1}{\sqrt{N!}}\ \det(\psi_i(\rho_j, \varphi_j, z_j)) \quad (2)$$

from single-electron orbitals which are expanded in the complete basis of Landau states, $\psi_i(\rho,\varphi,z) = \sum_{n=0}^{\infty} P_{ni}(z)\ \Phi_{ni}(\rho,\varphi)$, and to determine the longitudinal expansion functions self-consistently. Here we make the approximation that, for a given single-electron orbital, the expansion functions are identical for all Landau quantum numbers n, while every Landau level contributes with a different weight coefficient t_{in},

$$\psi_i(\rho,\varphi,z) = P_i(z) \sum_{n=0}^{N_{\rm L}} t_{in}\ \phi_{ni}(\rho,\varphi)\,. \quad (3)$$

For practical reasons the expansion has to be cut off at some maximum Landau quantum number $N_{\rm L}$. This approximation is motivated by the fact that in calculations in the Landau basis for the hydrogen atom in a strong magnetic field the overall character of the longitudinal expansion functions was found to be identical in all Landau levels (cf. Fig. 4.3 in [10]). Note that in terms of the Landau states the form (3) is a true multi-configurational approach. As already mentioned the adiabatic approximation [14–17] is contained as a special case: The weights of all Landau levels are zero except for the lowest Landau level $n = 0$. The condition for the adiabatic approximation to be valid is $\beta_Z = B/B_Z \gg 1$, which has the intuitive meaning that the magnetic field is strong enough that the "gyration" of the electrons in the plane perpendicular to the magnetic field in quantized Landau orbits is "fast" compared with the oscillating motion of the electrons in the direction of the field, which is caused by the Coulomb attraction of the positively charged nucleus or core. By contrast our method will also cover the range of magnetic field parameters $\beta_Z \sim 1$, where the adiabatic approximation breaks down.

The self-consistent-field equations for determining the longitudinal wave functions $P_i(z)$ and the weights t_{in} of all orbitals i are obtained in the usual way by inserting the Slater determinant (2) with the orbitals (3) into the variational principle for the total energy. They are solved iteratively in a doubly self-consistent manner. In every iteration step, first the Landau weights are kept fixed and the longitudinal wave functions are obtained

by solving the Hartree-Fock equations. Then the longitudinal wave functions are kept fixed and new Landau weights are determined by solving the Hartree-Fock-Roothaan equations. The iteration can be initialized by adiabatic approximation wave functions, i.e., with weight vectors $\mathbf{t}_i = (1, 0, 0, \dots)$, and simple forms for $P_i(z)$. We next describe the two procedures in more detail.

B. Hartree-Fock finite element (HFFE) procedure

In this step of the iteration all Landau weight coefficients are fixed, $t_{in} = \text{const}$, and the total energy is minimized with respect to the expansion functions. This yields the following system of Hartree-Fock equations for the longitudinal orbitals $P_i(z)$

$$\Big[-\frac{\mathrm{d}^2}{\mathrm{d}z^2} + \underbrace{\epsilon_i^{(\mathrm{L})} + V_i(z) - \epsilon_i + \sum_{\substack{j=1 \\ j\neq i}}^{N} Y_{ij}(z)}_{c_i(z)} \Big] P_i(z) = \underbrace{\sum_{\substack{j=1 \\ j\neq i}}^{N} P_j(z) X_{ij}(z)}_{h_i(z)} . \quad (4)$$

They manifestly depend on the Landau weights t_{in}. Specifically,

$$\epsilon_i^{(\mathrm{L})} = 4\beta \sum_{n=0}^{N_\mathrm{L}} (t_{in})^2 \, n \quad (5)$$

is the average single-particle Landau energy,

$$V_i(z) = \sum_{n,n'=0}^{N_\mathrm{L}} t_{in} t_{in'} V_i^{(n,n')}(z) \quad (6)$$

is the average single-particle potential, built from the effective Landau-Landau potentials

$$V_i^{(n,n')}(z) = -2\, Z \int \frac{\Phi_{ni}^*(\mathbf{r}^\perp)\; \Phi_{n'i}(\mathbf{r}^\perp)}{|\mathbf{r}|} \, \mathrm{d}\mathbf{r}^\perp , \quad (7)$$

and the direct and exchange potentials in (4) are given by

$$Y_{ij}(z) = \sum_{n,n',k,k'=0}^{N_\mathrm{L}} t_{in} t_{in'} t_{jk} t_{jk'} \; Y_{ij}^{(nk,n'k')}(z) \quad (8)$$

$$X_{ij}(z) = \sum_{n,n',k,k'=0}^{N_\mathrm{L}} t_{in} t_{in'} t_{jk} t_{jk'} \; X_{ij}^{(nk,n'k')}(z) \quad (9)$$

with

$$Y_{ij}^{(nk,n'k')}(z) = \int_{-\infty}^{\infty} (P_j(z'))^2 \times U_{ij}^{(nk,n'k')}(z,z') \, \mathrm{d}z' \quad (10)$$

$$X_{ij}^{(nk,n'k')}(z) = \int_{-\infty}^{\infty} P_i(z') \, P_j(z') \times A_{ij}^{(nk,n'k')}(z,z') \, \mathrm{d}z' \quad (11)$$

and the effective two-particle Landau-Landau direct and exchange potentials

$$U_{ij}^{(nk,n'k')}(z_1,z_2) = 2 \iint \frac{\Phi_{ni}^*(\mathbf{r}_1^\perp)\Phi_{kj}^*(\mathbf{r}_2^\perp)\Phi_{n'i}(\mathbf{r}_1^\perp)\Phi_{k'j}(\mathbf{r}_2^\perp)}{|\mathbf{r}_1 - \mathbf{r}_2|} \, \mathrm{d}\mathbf{r}_1^\perp \mathrm{d}\mathbf{r}_2^\perp , \quad (12)$$

$$A_{ij}^{(nk,n'k')}(z_1,z_2) = 2 \iint \frac{\Phi_{ni}^*(\mathbf{r}_1^\perp)\Phi_{kj}^*(\mathbf{r}_2^\perp)\Phi_{n'i}(\mathbf{r}_2^\perp)\Phi_{k'j}(\mathbf{r}_1^\perp)}{|\mathbf{r}_1 - \mathbf{r}_2|} \, \mathrm{d}\mathbf{r}_1^\perp \mathrm{d}\mathbf{r}_2^\perp , \quad (13)$$

respectively. The calculation of the potentials (6), (12), (13) is explained in the Appendix.

To solve the equations (4) we use finite elements and B-spline interpolation. The z-axis is divided into M finite elements with quadratically widening element borders,

$$I_m = [z_{m-1}, z_m] \quad \text{for} \quad m = 1, \dots, M \quad \text{with} \quad z_0 = 0 , \quad z_m = (m/M)^2 \, z_{\max} . \quad (14)$$

The quadratic widening accounts for the fact that the wave functions are richer in structure closer to the nucleus than further away from it. The longitudinal part of each single-particle orbital $\psi_i(\mathbf{r}) \equiv \phi_i(\rho,\varphi)\; P_i(z)$ is expanded in terms of B-splines of order k,

$$P_i(z) = \sum_l \alpha_l^{(i)} B_l(z). \quad (15)$$

They are polynomials of degree $k-1$ and represent a decomposition of the unity on the interpolation interval (cf. [18, 19]). The advantage of using B-splines, as opposed to Lagrange or Hermite interpolation, lies in their global definition on the interval $[0, z_{\max}]$. For illustration Fig. 1 shows an example of a complete quadratic ($k = 3$) B-spline basis set for quadratically widening element borders. The outer edges of the interpolation interval have to be considered as k multiple nodes to guarantee the $(k-2)$ times continuous differentiability over the interpolation interval.

The sequence of nodes defined by (14) does not belong to the class of quasi-uniform grids, which have proved advantageous in calculations using finite-difference approximations for differentiation operators (see, e.g., [20–22]).

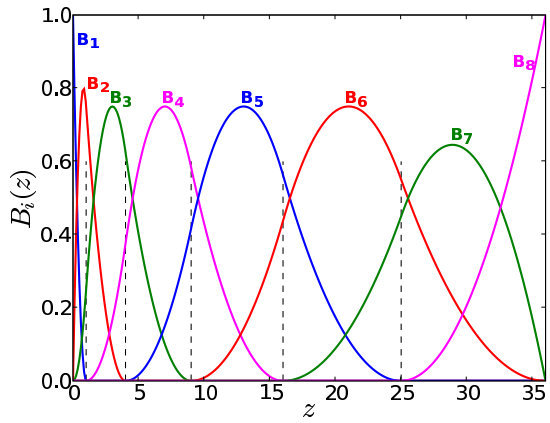

FIG. 1: Complete quadratic ($k = 3$) B-spline basis sets for interpolation in the interval $[0, 36]$ with quadratically widening nodes. The vertical dashed lines indicate the positions of the nodes. The borders of the complete interpolation interval are triple nodes.

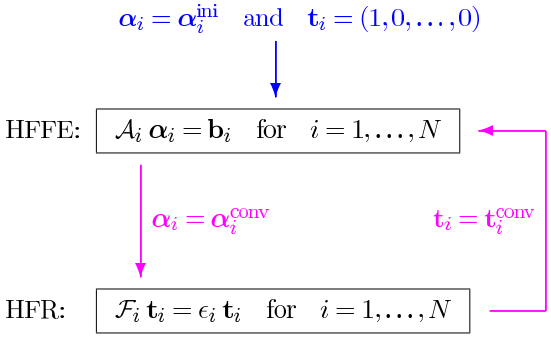

FIG. 2: Simplified flow diagram of the HFFER algorithm. In the HFFE stage the Hartree-Fock equations are solved to determine the B-spline expansion coefficient vectors $\boldsymbol{\alpha}_i$ of the orbitals. The converged values $\boldsymbol{\alpha}_i^{\rm conv}$ are handed over to the HFR stage, where the Hartree-Fock-Roothaan equations are solved to obtain new converged Landau weights $\mathbf{t}_i^{\rm conv}$, which in turn serve as "frozen" input for the next HFFE stage of the iteration. Both the HFFE and the HFR stage are MPI parallelized. Adiabatic approximation wave functions coefficients $\boldsymbol{\alpha}_i^{\rm ini}$ enter the initial HFFE iteration, with $\mathbf{t}_i^{\rm ad} = (1, 0, 0, \ldots)$.

This circumstance, however, does not affect adversely the present finite-element calculations using B-splines, which can be differentiated analytically, and therefore no discretization of differentiation operators is required.

The task of finding self-consistent solutions of the Hartree-Fock equations (4) is now reduced to determining the expansion coefficients $\alpha_l^{(i)}$ for the N single-electron orbitals $P_i(z)$. Expressing the total energy as as a real-valued function of all expansion coefficients and minimizing with respect to the expansion coefficients leads to the system of inhomogeneous linear equations

$$\mathcal{A}_i\,\boldsymbol{\alpha}_i = \mathbf{b}_i \quad \text{for} \quad i = 1,\ldots,N\,, \tag{16}$$

with the matrices

$$\begin{aligned}(\mathcal{A}_i)_{kl} \;=\; & \sum_{m=1}^{M} \Bigg[\int_{I_m} B_k'(z) B_l'(z) \\ & +\; c_i(z) B_k(z) B_l(z)\,\mathrm{d}z \Bigg] \end{aligned} \tag{17a}$$

and the vectors

$$(\mathbf{b}_i)_k = \sum_{m=1}^{M} \Bigg[\int_{I_m} h_i(z) B_k(z)\,\mathrm{d}z \Bigg]\,. \tag{17b}$$

The functions $c_i(z)$ and $h_i(z)$ are defined in the Hartree-Fock equations (4).

In our calculations, we use sixth-order B-splines and typically 15–20 finite elements. The maximum integration radius $z_{\rm max}$ is chosen such that all longitudinal wave functions have decayed exponentially ($z_{\rm max} \sim 2 - 30$ atomic units).

C. Hartree-Fock-Roothaan (HFR) procedure

In the Hartree-Fock-Roothaan step all longitudinal wave functions are kept fixed and new Landau weight coefficients are determined by minimizing the energy functional with respect to the coefficients. This leads to the Hartree-Fock-Roothaan equations

$$\mathcal{F}_i\,\mathbf{t}_i = \epsilon_i\,\mathbf{t}_i \quad \text{for} \quad i = 1,\ldots,N\,, \tag{18}$$

where the matrices $\mathcal{F}_i$ are composed of five contributions,

$$\begin{aligned}(\mathcal{F}_i)_{nn'} \;=\; & (\mathcal{F}_i^{(\mathrm{L})})_{nn'} + (\mathcal{F}_i^{(\mathrm{K})})_{nn'} \\ & +\; (\mathcal{F}_i^{(\mathrm{V})})_{nn'} + (\mathcal{F}_i^{(\mathrm{Y})})_{nn'} \\ & +\; (\mathcal{F}_i^{(\mathrm{X})})_{nn'}\,. \end{aligned} \tag{19}$$

The five terms represent, in this order, the Landau energy, the kinetic energy of the longitudinal motion, the effective potential of the nucleus and the direct and the exchange potentials,

$$(\mathcal{F}_i^{(\mathrm{L})})_{nn'} \;=\; 4\beta n \,\cdot\, \delta_{nn'} \tag{20a}$$

$$(\mathcal{F}_i^{(\mathrm{K})})_{nn'} \;=\; \int_{-\infty}^{\infty} (P_i'(z))^2\,\mathrm{d}z \,\cdot\, \delta_{nn'} \tag{20b}$$

$$(\mathcal{F}_i^{(\mathrm{V})})_{nn'} \;=\; \int_{-\infty}^{\infty} (P_i(z))^2\; V_i^{(n,n')}(z)\,\mathrm{d}z \tag{20c}$$

$$(\mathcal{F}_i^{(\mathrm{Y})})_{nn'} = \sum_{\substack{j=1\\ j\neq i}}^{N} \sum_{k,k'=0}^{N_\mathrm{L}} t_{jk}\, t_{jk'} \times \int_{-\infty}^{\infty} (P_i(z))^2\, Y_{ij}^{(nk,n'k')}(z)\,\mathrm{d}z \quad (20\mathrm{d})$$

$$(\mathcal{F}_i^{(\mathrm{X})})_{nn'} = -\sum_{\substack{j=1\\ j\neq i}}^{N} \sum_{k,k'=0}^{N_\mathrm{L}} t_{jk}\, t_{jk'} \times \int_{-\infty}^{\infty} P_j(z)P_i(z)\, X_{ij}^{(nk,n'k')}(z)\,\mathrm{d}z\,. \quad (20\mathrm{e})$$

Since the matrices depend on the Landau weights, the equations (18) have to be solved iteratively, using the weights of the previous step for constructing the matrices to determine new Landau weights, until convergence is achieved. The converged Landau weights then enter into the next Hartree-Fock-Finite-Element stage of the calculation. The convergence criterion in both the HFR and the HFFE stage is that the absolute energy values between two successive iteration steps differ by less than 1.0×10^{-5} keV.

A schematic flow chart of the complete Hartree-Fock-Finite-Element-Roothaan procedure is shown in Fig. 2.

D. Choice of initial wave functions

The calculation is initialized by setting all Landau weights to $\mathbf{t}_i = (1, 0, 0, \dots)$, and distributing the electrons on magnetic sublevels according to the level scheme of the hydrogen atom in intense magnetic fields. As simple initial longitudinal wave functions we choose the approximate wave functions of the hydrogen atom in a strong magnetic field suggested by Canuto and Kelly [23]. They have the advantage that they can be expressed in analytical form. According to the level scheme one has to distinguish between "tightly bound" and "hydrogen-like" states.

1. *Tightly bound states*

For tightly bound states, with number of nodes $\nu = 0$, and magnetic quantum numbers $m \leq 0$, Gaussian type orbitals

$$P_m(z) \propto \exp\left(-\frac{\lambda_m^2}{2}\frac{z^2}{a_\mathrm{L}^2}\right) \quad (21)$$

are adopted whose widths λ_m are gained by minimizing the expectation value of the Hamiltonian of the hydrogen atom in a magnetic field. This leads to the transcendental equation

$$\lambda_m = \frac{4\,a_\mathrm{L}}{a_0\sqrt{\pi}}\left[\ln\left(\frac{2}{\lambda_m}\right) - 1 - \frac{1}{2}A_m\right] \quad (22)$$

$$\text{with} \quad A_0 := 0 \quad \text{and} \quad A_m := \sum_{k=1}^{-m}\frac{1}{k} \quad \text{for} \quad m \leq -1,$$

which in the code is solved numerically using the Brent method [24]. The magnetic field dependence is contained in the Larmor radius $a_\mathrm{L} = a_0/\sqrt{\beta}$.

2. *Hydrogen-like states*

The effective potentials $V_{|m|}(z)$, obtained by averaging the electron-nucleus interaction over the Landau state $\phi_{0m}(\mathbf{r}_\perp)$, have finite values and a cusp at $z = 0$, and behave as $1/|z|$ for large z. They can be modeled by truncated Coulomb potentials $V_{|m|} \propto 1/(|z| + d_m)$. For excited states, with quantum numbers $m \leq 0, \nu > 0$ ("hydrogenlike" states) we therefore choose as initial wave functions solutions of the one-dimensional Schrödinger equation with these potentials, which are Whittaker functions $W_{\alpha,\frac{1}{2}}$

$$P_m(z) \propto W_{\alpha_m,\frac{1}{2}}(\zeta) \quad \text{with} \quad \zeta := \frac{2z}{\alpha_m a_0} + \frac{2d_m}{\alpha_m a_0}\,. \quad (23)$$

The width parameters d_m and the parameter α_m follow from the condition that the expectation values of the exact Coulomb potential and the truncated Coulomb potential conincide.

For excited states with negative z parity (odd number of nodes $\nu = 2p - 1$) this leads to [23]

$$\alpha_m^{\mathrm{odd}} = p + \frac{2\,d_m^{\mathrm{odd}}}{a_0} \quad \text{with} \quad p = 1, 2, \dots\,, \quad (24\mathrm{a})$$

$$d_m^{\mathrm{odd}} = \frac{p\,a_0}{\lambda_m}\left[\ln(\lambda_m) - 1\right],\ \lambda_m = \frac{4\,p^2 a_0^2}{(1-m)\,a_\mathrm{L}^2}, \quad (24\mathrm{b})$$

while for excited states with positive z parity (even number of nodes $\nu = 2p$) one has

$$\alpha_m^{\mathrm{even}} = p + \frac{1}{t_m + \sqrt{t_m^2 + \frac{\pi^2}{3}}} \quad \text{with} \quad p = 1, 2, \dots,$$

$$\text{and} \quad t_m = -0.58 - \frac{d_m^{\mathrm{even}}}{a_0} - \frac{1}{2}\ln\left(\frac{2\,d_m^{\mathrm{even}}}{a_0}\right) + \frac{1}{24p^2}\,, \quad (25\mathrm{a})$$

$$d_m^{\mathrm{even}} = \sqrt{\frac{1-m}{\gamma}}\,\frac{a_\mathrm{L}}{2}\,, \quad (25\mathrm{b})$$

with $\gamma \approx 0.577$ the Euler-Mascheroni constant. The magnetic field dependence of the length parameters d_m again

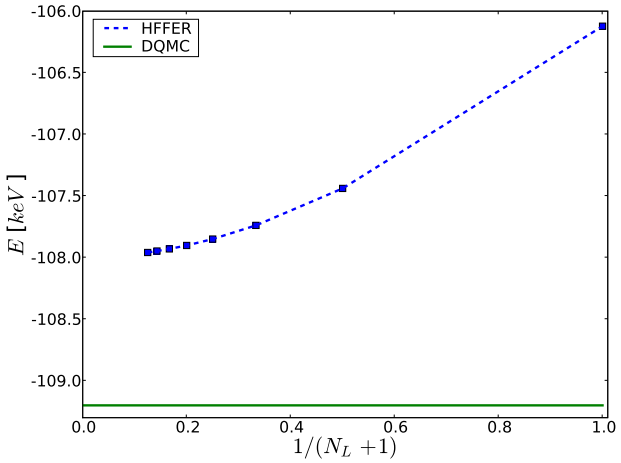

FIG. 3: Energy values obtained by the HFFER procedure as a function of the inverse number of Landau levels considered, for the ground state of neutral iron at $B = 5 \times 10^8$ T. The value at $1/(N_\mathrm{L}+1) = 1$ corresponds to that of the adiabatic approximation. For comparison the very accurate result of a DQMC calculation [9] is shown by the horizontal line. It is seen that the HFFER values saturate at $E \approx -108.0$ keV. The remaining error with regard to the DQMC result is the consequence of our approximation (3).

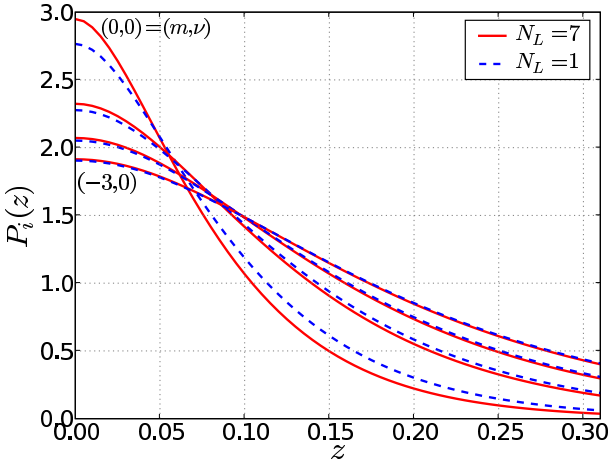

FIG. 4: Comparison between the longitudinal orbitals obtained in adiabatic approximation, and with 8 Landau channels for the ground state of neutral silicon at $B = 1.0 \times 10^8$ T (four innermost electrons). Note the increase of the wave function amplitude close to the nucleus for $N_\mathrm{L} = 7$.

is contained in the Larmor radius. The Whittaker functions are represented numerically by confluent hypergeometric functions $U(a, b, x)$ which are evaluated in the code using the algorithm of [25].

The only free parameter a_0 determines the extension of the initial wave functions. For tightly bound states $a_0 = 1/Z$ turned out to be a good choice. In many cases even and odd initial wave functions with $a_0 = 1$ yield converging results. In other cases values $a_0 < 1$ must be varied separately for even and odd states to achieve convergence.

III. RESULTS AND DISCUSSION

To speed up the calculations both the Hartree-Fock-Finite-Element procedure and the Hartree-Fock-Roothaan procedure were parallelized using the MPI (message passing interface) library . Typically each MPI process deals with one electron. For 26 MPI processes this results in a run time of less than 500 seconds for the ground state of iron at $B = 5 \times 10^8$ T. The parallelization efficiency was about 80 per cent. Our calculations were performed on the cacau cluster of the High Performance Computing Center Stuttgart (HLRS), where we used up to 13 double-processor nodes (3.2 GHz, 1 GByte RAM per node).

A typical example for the convergence behavior of the HFFER procedure with increasing number N_L of Landau channels is shown in Fig. 3 for the ground state of neutral iron at a magnetic field strength of 5×10^8 T. This corresponds to a magnetic field parameter of $\beta_Z \approx 1.57$ for which the adiabatic approximation should be poor. Indeed it can be seen that the energy value in adiabatic aprroximation ($N_\mathrm{L} = 0$) is already considerably lowered if only one more Landau level is taken into account. With increasing number of Landau channels the energy runs into a regime of saturation at $E \approx 108.0$ keV. For comparison, Fig. 3 contains the result of a recent highly accurate DQMC calculation [9]. Compared with the adiabatic approximation energy value the HFFER procedure reduces the error with respect to the DQMC result by a factor of three (reduction to 1/3 of the original error). The remaining deviation from the correct energy value is less than 1 per cent, and a consequence of our approximation (3).

For the ground state of silicon at $B = 1.0 \times 10^8$ T ($\beta_Z \approx 1.1$) Table I lists converged single-particle energy values of the HFFER procedure and the Landau weights for the two lowest and the highest Landau channel considered in our calculations. The adiabatic approximation result $E = -18616$ eV is improved to $E = -19176$ eV by taking 8 Landau channels into account. It can be recognized from the single-particle energies that it is the innermost electrons which contribute to the lowering of the energy because they possess a relatively large first Landau weight coefficient t_1. The corrections stemming from the higher Landau quantum numbers are seen to be small. For the 4 innermost electrons (magnetic quantum numbers $m = 0, -1, -2, -3$) Fig. 4 shows a comparison between the longitudinal wave functions obtained in adiabatic approximation, and with 8 Landau channels. It is evident that the energy lowering follows from the increase of the wave function amplitude in the vicinity of

the nucleus.

TABLE I: Single-particle energies ϵ in adiabatic approximation ($N_\mathrm{L} = 0$) and with 8 Landau channels ($N_\mathrm{L} = 7$), and Landau weights t_0, t_1, and t_7 for the ground state of neutral silicon at $B = 1.0 \times 10^8$ T.

		$N_\mathrm{L} = 0$ ($E = -18618$ eV)	$N_\mathrm{L} = 7$ ($E = -19176$ eV)			
m	ν	ϵ/eV	ϵ/eV	t_0	t_1	t_7
0	0	−3279.5	−3692.6	0.98446	0.15886	0.00699
-1	0	−1580.2	−1632.8	0.99710	0.07183	0.00146
-2	0	−1016.7	−1028.9	0.99896	0.04360	0.00053
-3	0	−730.23	−733.28	0.99952	0.02977	0.00024
-4	0	−557.90	−558.29	0.99975	0.02157	0.00012
-5	0	−444.52	−444.07	0.99986	0.01620	0.00007
-6	0	−365.57	−364.90	0.99992	0.01246	0.00004
-7	0	−308.20	−307.54	0.99995	0.00977	0.00003
-8	0	−264.81	−264.23	0.99997	0.00781	0.00002
-9	0	−230.34	−229.87	0.99998	0.00638	0.00001
-10	0	−200.89	−200.52	0.99999	0.00533	0.00001
0	1	−195.17	−187.08	0.99989	0.01429	0.00008
-11	0	−172.45	−172.17	0.99999	0.00455	0.00001
-12	0	−137.67	−137.46	0.99999	0.00389	0.00001

We now present numerical results obtained by the HFFER method with 8 Landau channels and compare them with both the results in adiabatic approximation ($N_\mathrm{L} = 0$) and the results of other methods. Table II lists the ground state energies of the neutral atoms from helium to silicon at 5×10^7 T (corresponding to the magnetic field parameter range $\beta_{Z=2} = 26.6$ to $\beta_{Z=14} = 0.543$). The numbers in brackets designate the number of electrons occupying an excited hydrogen-like single-particle longitudinal state. The improvement on the energy values in the adiabatic approximation is evident, in particular for higher Z, where the β_Z values become of the order of unity. As reference values the results of the diffusion quantum Monte Carlo calculation (DQMC) [9] are listed. The DQMC values are presently the most accurate energy values available, since their calculation practically involves no restricting approximations. Compared with these values the absolute error of the adiabatic approximation energies shrinks by roughly one third for helium, and by two thirds for silicon (the relative deviation is 1.1 per cent for helium and 2.1 per cent for silicon). Deviations of this order as compared with the DQMC results have been found typical of the HFFER results with $N_\mathrm{L} = 7$.

For comparison Table II also contains literature values obtained by Ivanov and Schmelcher [26] using a two-dimensional Hartree-Fock method (2DHF), by Mori and Hailey [6] (MCPH^3, multi-configurational perturbative hybrid Hartree-Hartree-Fock), and the results of an older 1DHF (one-dimensional Hartree-Fock) calculation [15]. The 1DHF results should conincide with the energies calculated in adiabatic approximation ($N_\mathrm{L} = 0$) but are clearly seen to lie above them. This suggests that the old 1DHF results were numerically flawed. While the 2DHF method is an ab-initio method, the MCPH^3 method is not, since it evaluates the exchange energy in first-order perturbation theory in a basis of Hartree states obtained in adiabatic approximation, and it does not include the back-reaction of the excited Landau states, whose weights are taken into account perturbatively, on the effective interaction potentials. Therefore the method need not necessarily produce an upper bound on the energy. This may explain why for large nuclear charges the MCPH^3 results also fall below the accurate DMQC values ($Z = 12 - 14$ in Table II).

This behavior is even more conspicuous in Table III where the ground state energies of the neutral atoms from helium up to iron are given for the magnetic field strength of 1×10^8 T (corresponding to the range from $\beta_{Z=2} = 53.2$ to $\beta_{Z=26} = 0.315$). Compared with the DQMC value for the ground state energy of iron the HFFER method reduces the relative deviation of the adiabatic calculation from 7.2 per cent to 2.0 per cent.

The ground state energies for helium up to iron at $B = 5 \times 10^8$ T are given in Table IV (range from $\beta_{Z=2} = 266$ to $\beta_{Z=26} = 1.57$). Here the HFFER method reduces the error for iron from 2.7 per cent (adiabatic) to 1.0 per cent (nonadiabatic).

Compared with the DQMC method the HFFER method has two essential advantages. Firstly it includes both the calculation of energies and wave functions and thus allows for the calculation of electromagnetic transition rates. Secondly the computing times required are considerably shorter. For the ground state of neutral iron at $B = 5 \times 10^8$ T (example of Fig. 3) the parallelized execution of the DQMC method on a 26 processor cluster takes 8.6 hours, while the parallelized HFFER code with 8 Landau channnels on the same cluster only runs 463 seconds. This is 67 times faster than the DQMC run, and only by a factor of 5.4 longer than the run time of the simple adiabatic calculation of 85 seconds. This clearly demonstrates that the HFFER method is optimally adapted to the fast and routine calculation of atomic data with sufficient numerical accuracy in neutron star magnetic fields.

We now proceed to results for oscillator strengths of electromagnetic transitions. As an example Table V shows the oscillator strengths for transitions between the carbon ground state and an excited state in which one electron is raised from a nodeless to a one-node orbital. Three magnetic field strengths for which comparison values exist in the literature are considered, corresponding to values of the magnetic field parameter $\beta = 200,\ 500,\ 1000$ ($\beta_{Z=6} = 5.6,\ 13.9,\ 27.8$). Results are shown for $N_\mathrm{L} = 7$ and for the adiabatic approximation, and compared with the values given by Mori and Hailey [6] (MCPH^3). It must be noted that the latter values were corrected by the authors on account of the not highly accurate longitudinal Hartree wave functions by an auxiliary factor. It can be seen that the oscillator strengths are comparable in magnitude but deviations

TABLE II: Energy values in keV for the ground states of the neutral atoms from helium to silicon at $B = 5.0 \times 10^7$ T. ($N_\mathrm{L} = 0$: adiabatic approximation; $N_\mathrm{L} = 7$: HFFER method with 8 Landau channels; DQMC: released phase diffusion quantum Monte Carlo [9]; MCPH^3: multi-configurational perturbative hybrid Hartree-Hartree-Fock [6]; 2DHF: two-dimensional Hartree-Fock [26]; 1DHF: one-dimensional Hartree-Fock [15]). Numbers in brackets designate the number of electrons occuping a one-node excited orbital, all other electrons are in a tightly bound state.

Z	$N_\mathrm{L} = 7$	$N_\mathrm{L} = 0$	DQMC	MCPH^3	2DHF	1DHF
2	−0.4575	−0.4551	−0.4626	−0.4567	−0.46063	−0.454
3	−0.9538	−0.9458	−0.9661	−0.9526	−0.96180	−0.944
4	−1.601	−1.582	−1.622	−1.600	−1.61624	−1.580
5	−2.386	−2.349	−2.421	−2.390	−2.41101	−2.347
6	−3.299	−3.237	−3.349	−3.308	−3.33639	−3.22
7	−4.333	−4.234	−4.402	−4.353	−4.38483	−4.22
8	−5.481	−5.336	−5.573	−5.517	−5.55032	−5.32
9	−6.739	−6.534	−6.857	−6.803	−6.82794	−6.51
10	−8.102	−7.825	−8.250	−8.198	−8.21365	−7.819
11	−9.566	−9.204	−9.752	−9.718		−9.197
12	−11.182(1)	−10.728(1)	−11.400	−11.410(1)		−10.72(1)
13	−12.898(1)	−12.330(1)	−13.163	−13.251(1)		−12.32(1)
14	−14.712(2)	−14.019(2)	−15.031	−15.246(2)		−14.00(1)

TABLE III: Energy values in keV for the ground states of the neutral atoms from helium to iron at $B = 1.0 \times 10^8$ T. Designations as in Table II.

Z	$N_\mathrm{L} = 7$	$N_\mathrm{L} = 0$	DQMC	MCPH^3	2DHF	1DHF
2	−0.5771	−0.5753	−0.5827	−0.5766	−0.57999	−0.574
3	−1.217	−1.211	−1.230	−1.214	−1.22443	−1.209
4	−2.059	−2.044	−2.081	−2.056	−2.07309	−2.042
5	−3.085	−3.057	−3.122	−3.085	−3.10924	−3.054
6	−4.284	−4.236	−4.338	−4.288	−4.31991	−4.20
7	−5.645	−5.568	−5.716	−5.657	−5.69465	−5.54
8	−7.159	−7.045	−7.252	−7.176	−7.2249	−7.02
9	−8.818	−8.658	−8.938	−8.845	−8.90360	−8.63
10	−10.617	−10.400	−10.766	−10.664	−10.72452	−10.39
11	−12.551	−12.265	−12.725	−12.625		−12.25
12	−14.615	−14.248	−14.827	−14.745		−14.23
13	−16.803(1)	−16.351(1)	−17.061	−16.973(1)		−16.34(1)
14	−19.176(1)	−18.618(1)	−19.480	−19.408(1)		−18.60(1)
15	−21.678(1)	−21.001(1)	−22.022	−21.987(1)		−20.95(1)
16	−24.286(2)	−23.480(2)	−24.700	−24.718(2)		−23.43(2)
17	−27.083(2)	−26.129(2)	−27.541	−27.618(2)		−26.07(2)
18	−30.008(2)	−28.889(2)	−30.529	−30.766(2)		−28.82(2)
19	−33.056(2)	−31.755(2)	−33.650	−34.036(2)		
20	−36.243(3)	−34.750(3)	−36.891	−37.500(3)		
21	−39.574(3)	−37.866(3)	−40.296			
22	−43.026(3)	−41.084(3)	−43.867			
23	−46.617(4)	−44.427(4)	−47.526			
24	−50.342(4)	−47.881(4)	−51.360			
25	−54.179(5)	−51.432(5)	−55.279			
26	−58.167(5)	−55.111(5)	−59.366	−55.410(5)[c]		−55.10(6)

from the adiabatic approximation results and those obtained with MCPH^3 appear in particular in excitations at intermediate magnetic quantum numbers.

The HFFER method aims at the calculation of large atoms and ions in intense magnetic fields. As an example, Table VI shows results for iron ions with 5 (FeXXI) to 25 (FeII) electrons in a magnetic field of 5×10^8 T. The table lists the energies of the ground state and an excited state in which the electron with the maximum modulus of the magnetic quantum number is raised into a one-node orbital, while all other electrons successively occupy nodeless orbitals with decreasing m. In addition, the oscillator strengths of transitions from the excited to the ground states are given. To emphasize the improvement

TABLE IV: Energy values in keV for the ground states of the neutral atoms from helium to iron at $B = 5.0\times10^8$ T. Designations as in Table II.

Z	$N_\mathrm{L}=7$	$N_\mathrm{L}=0$	DQMC	MCPH^3	2DHF	1DHF
2	−0.9596	−0.9589	−0.9664	−0.9574	−0.96191	−0.9580
3	−2.083	−2.080	−2.103	−2.078	−2.08931	−2.0760
4	−3.598	−3.591	−3.630	−3.586	−3.61033	−3.5840
5	−5.479	−5.465	−5.525	−5.478	−5.49950	−5.4560
6	−7.704	−7.679	−7.766	−7.695	−7.73528	−7.60
7	−10.254	−10.214	−10.343	−10.231	−10.29919	−10.20
8	−13.115	−13.054	−13.224	−13.099	−13.17543	−13.00
9	−16.272	−16.185	−16.412	−16.264	−16.34997	−16.10
10	−19.712	−19.592	−19.881	−19.702	−19.81072	−19.57
11	−23.425	−23.267	−23.635	−23.406		−24.64
12	−27.402	−27.197	−27.655	−27.436		−27.17
13	−31.633	−31.374	−31.931	−31.675		−31.35
14	−36.111	−35.789	−36.442	−36.154		−35.74
15	−40.829	−40.435	−41.203	−40.915		−40.35
16	−45.780	−45.306	−46.214	−45.881		−45.22
17	−50.957	−50.393	−51.445	−51.067		−50.30
18	−56.356	−55.693	−56.894	−56.530		−55.95
19	−61.971	−61.198	−62.584	−62.181		
20	−67.798	−66.904	−68.447	−68.031		
21	−73.919(1)	−72.902(1)	−74.669	−74.184(1)		
22	−80.275(1)	−79.116(1)	−81.071	−80.602(1)		
23	−86.844(1)	−85.533(1)	−87.633	−87.263(1)		
24	−93.623(1)	−92.146(1)	−94.561	−94.259(1)		
25	−100.61(1)	−98.952(1)	−101.615	−101.25(1)		
26	−107.96(2)	−106.13(2)	−109.079	−108.64(2)		−106.09(2)

TABLE V: Oscillator strengths of transitions to the carbon ground state at three values of the magnetic field parameter β. The transitions occur between the orbitals $(m^*,0)\leftrightarrow(m^*,1)$, all other other electrons remain in their nodeless orbitals $(m,0)$. $N_\mathrm{L}=0$: adiabatic approximation; $N_\mathrm{L}=7$: HFFER with 8 Landau channels; MCPH^3: results of Ref. [6].

	$\beta=200$			$\beta=500$			$\beta=1000$		
$(m,\nu)\leftrightarrow(m',\nu')$	$N_\mathrm{L}=7$	$N_\mathrm{L}=0$	MCPH^3	$N_\mathrm{L}=7$	$N_\mathrm{L}=0$	MCPH^3	$N_\mathrm{L}=7$	$N_\mathrm{L}=0$	MCPH^3
$(0,0)\leftrightarrow(0,1)$	0.0416	0.0477	0.0410	0.0118	0.0126	0.0130	0.00603	0.00628	0.00581
$(-1,0)\leftrightarrow(-1,1)$	0.0675	0.0708	0.0598	0.0264	0.0270	0.0225	0.0150	0.0152	0.0128
$(-2,0)\leftrightarrow(-2,1)$	0.0988	0.101	0.0797	0.0447	0.0450	0.0392	0.0268	0.0268	0.0247
$(-3,0)\leftrightarrow(-3,1)$	0.135	0.136	0.114	0.0667	0.0668	0.0611	0.0413	0.0412	0.0377
$(-4,0)\leftrightarrow(-4,1)$	0.172	0.172	0.156	0.0917	0.0916	0.0863	0.0585	0.0584	0.0572
$(-5,0)\leftrightarrow(-5,1)$	0.205	0.205	0.197	0.119	0.119	0.116	0.0794	0.0792	0.0783

over the adiabatic approximation, the corresponding results for $N_\mathrm{L}=0$ are also tabulated. Finally ground state energy values of the DQMC calculation are also shown. It can be seen that the relative deviation of the ground state energies from the DQMC values are reduced from 6.8 per cent (adiabatic) to 2.0 per cent (nonadiabatic) for FeXXI, and from 2.6 per cent to 0.9 per cent for FeII.

Oscillator strengths are found to be very large when in the ground state none of the electrons occupies a one-node orbital ($N=5-11$). If in the ground state configuration electrons occupy orbitals with one node the oscillator strengths are generally much smaller because of less overlap between the two states. The relative corrections of the oscillator strengths in adiabatic approximation by the HFFER results are large in particular for transitions with small oscillator strengths (up to ~ 50 per cent for the entries with $N\geq 20$), while for large oscillator strengths the adiabatic calculation yields a good approximation. This may be due to the fact that the errors in the energy values cancel when the the difference of the energy values is taken.

IV. CONCLUSIONS

In this paper we have introduced the Hartee-Fock-Finite-Element-Roothaan method. We have demonstrated that it is a powerful tool with which the energies

TABLE VI: Iron ions with $5 \le N \le 25$ electrons: ground state energies E in keV, energies of excited states E^* in keV, and oscillator strengths f at $B = 5.0 \cdot 10^8$ T. In the excited states the electron with the highest $|m|$ is raised to a $\nu = 1$ orbital, the others occupy a nodeless orbital. For the ground states, the number of electrons in one-node orbitals is added in brackets. HFFER ($N_\mathrm{L} = 7$) values are compared with the corresponding adiabatic ($N_\mathrm{L} = 0$) results. The last column contains the ground state energies computed by diffusion quantum Monte Carlo [9].

	$N_\mathrm{L} = 7$			$N_\mathrm{L} = 0$			DQMC
N	E	E^*	f	E	E^*	f	E
5	−58.267	−54.494	0.882	−56.455	−52.708	0.890	−59.141
6	−64.214	−60.973	0.891	−62.386	−59.161	0.896	−65.079
7	−69.466	−66.630	0.896	−67.629	−64.802	0.900	−70.362
8	−74.143	−71.627	0.899	−72.298	−69.790	0.902	−75.047
9	−78.327	−76.077	0.900	−76.478	−74.232	0.903	−79.250
10	−82.083	−80.056	0.899	−80.231	−78.207	0.902	−82.992
11	−85.459	−83.625	0.898	−83.604	−81.773	0.900	−86.375
12	−88.617(1)	−86.827	0.300	−86.773(1)	−84.986	0.216	−89.550
13	−91.469(1)	−89.848	0.312	−89.624(1)	−88.005	0.229	−92.401
14	−94.018(1)	−92.548	0.323	−92.172(1)	−90.703	0.241	−94.979
15	−96.291(1)	−94.957	0.333	−94.445(1)	−93.111	0.252	−97.238
16	−98.310(1)	−97.100	0.340	−96.463(1)	−95.253	0.261	−99.260
17	−100.09(1)	−98.997	0.346	−98.247(1)	−97.151	0.269	−101.06
18	−101.66(1)	−100.67	0.350	−99.811(1)	−98.822	0.275	−102.64
19	−103.02(1)	−102.13	0.351	−101.17(1)	−100.28	0.279	−104.00
20	−104.19(2)	−103.35	0.0758	−102.35(2)	−101.51	0.0487	−105.12
21	−105.22(2)	−104.48	0.0822	−103.39(2)	−102.64	0.0552	−106.19
22	−106.08(2)	−105.43	0.0858	−104.24(2)	−103.59	0.0599	−107.08
23	−106.77(2)	−106.22	0.0841	−104.93(2)	−104.38	0.0607	−107.70
24	−107.31(2)	−106.85	0.0721	−105.47(2)	−105.01	0.0541	−108.26
25	−107.70(2)	−107.34	0.0447	−105.86(2)	−105.51	0.0345	−108.70

and wave functions of ground states and excited states of many-electron atoms and ions in neutron star magnetic field strengths can be calculated. It also allows the calculation of oscillator strengths of bound-bound transitions between the states.

We have not considered relativistic effects, which are expected to be on the order of $(Z\alpha)^2$, and the effects of the finite nucleus mass. These effects are small compared with the observational uncertainties of spectral features and the smearing of spectral lines by the variation of the magnetic field across the neutron star's atmosphere.

The method is the first which systematically takes into account the influence of higher Landau channels on both energy values and oscillator strengths, and is superior to previous calculations using the adiabatic approximation or variants of it, at only a moderately higher computational expense. The method strikes a balance between numerical accuracy and computing times. It is therefore well adapted to routine computatons of the atomic data required by astronomers for their calculations of synthetic spectra of model atmospheres of magnetized neutron stars.

Calculations of extensive tables of atomic data in neutron star magentic fields using the HFFER method presented in this paper are under way.

Acknowledgments

This work was supported by Deutsche Forschungsgemeinschaft within the SFB 382 "Methods and Algorithms for Simulating Physical Processes on High-Performance Computers" at the Universities of Tübingen and Stuttgart. We thank V. Melezhik for a helpful discussion on quasi-uniform grids.

Appendix: Effective potentials

The calculation of the effective potentials (6), (12), (13) resorts to the method developed by Pröschel et al. [27]. The effective potentials can all be expanded in terms of the expectation values of the Coulomb potential with respect to the Landau states in the lowest Landau level and with different magnetic quantum numbers $m_i = -s$ ($s = 0, 1, 2, \dots$), which are given by the z-dependent functions

$$\tilde{V}_s(z) = \frac{1}{s!} \int_0^\infty \frac{x^s \mathrm{e}^{-x}}{\sqrt{x + z^2}} \, \mathrm{d}x \,. \tag{A.1}$$

The expansions read

$$V_i^{(n,n')}(z) = -2Z\sqrt{\beta}\sum_{s=|m_i|}^{n+n'-m_i} b_{is}^{(n,n')} \times \tilde{V}_s(\sqrt{\beta}\,z) \quad (A.2)$$

$$U_{ij}^{(nk,n'k')}(z_1,z_2) = \sqrt{2\beta}\sum_{s=0}^{q} c_{ijs}^{(nk,n'k')} \times \tilde{V}_s(\sqrt{\beta/2}\,|z_1-z_2|) \quad (A.3)$$

$$A_{ij}^{(nk,n'k')}(z_1,z_2) = \sqrt{2\beta}\sum_{s=0}^{q} d_{ijs}^{(nk,n'k')} \times \tilde{V}_s(\sqrt{\beta/2}\,|z_1-z_2|) \quad (A.4)$$

with $q = n + k + n' + k' - m_i - m_j$.

The expansion coefficients are given by [27]

$$b_{is}^{(n,n')} = \sqrt{\frac{(n-m_i)!(n'-m_i)!}{n!n'!}}\,\frac{(-1)^{s+|m_i|}\,s!}{(s+|m_i|)!} \times \sum_{\substack{k=0\\ k+k'=s-|m_i|}}^{n}\sum_{k'=0}^{n'} \binom{n}{k}\binom{n'}{k'}\binom{s+|m_i|}{k+|m_i|} \quad (A.5)$$

$$c_{ijs}^{(nk,n'k')} = \tilde{c}(n-m_i,k-m_j,n'-m_i,k'-m_j;n,k,n',k';s) \quad (A.6)$$

$$d_{ijs}^{(nk,n'k')} = \tilde{c}(n-m_i,k-m_j,k'-m_j,n'-m_i;n,k,k',n';s), \quad (A.7)$$

where the auxiliary functions $\tilde{c}$ are defined by

$$\tilde{c}(s_1,s_2,s_1',s_2';n_1,n_2,n_1',n_2';s) = \frac{1}{s!}\sqrt{\frac{s_1'!s_2!n_1'!n_2!}{s_1!s_2'!n_1!n_2'!}}\sum_{i,j,k,l}\left[\left(\frac{1}{2}\right)^{q-i-j-k-l}\frac{(-1)^{(s_1'-i)+(s_2-j)+(n_1'-k)+(n_2-l)}}{(s_1'-i)!\,(s_2-j)!\,(n_1'-k)!\,(n_2-l)!} \times\binom{s_1}{i}\binom{s_2'}{j}\binom{n_1}{k}\binom{n_2'}{l}\,(q-i-j-k-l)!\,(i+j+k+l-q)_s\right]. \quad (A.8)$$

In (A.8) in the second-last bracket the integer q is given by $q = (n_1+n_2+n_1'+n_2'+s_1+s_2+s_1'+s_2')/2$, and the last bracket with a subscript denotes a Pochhammer symbol (rising factorial) defined by $(x)_n = x\cdot(x+1)\cdots(x+n-1)$. Finally, the summation boundaries in the quadruple sum are: $i = 0,\ldots,\min(s_1,s_1')$, $j = 0,\ldots,\min(s_2,s_2')$, $k = 0,\ldots,\min(n_1,n_1')$, $l = 0,\ldots,\min(n_2,n_2')$.

In this work, the b, c and d coefficients were computed separately for 8 Landau channels ($0 \le n \le N_{\rm L} = 7$) for the magnetic quantum numbers $m = 0$ to $m = -25$ with an accuracy of 25 decimal digits and stored in data and pointer fields. At each program call the fields necessary for a given configuration were read in. The coefficients are distributed over the cluster nodes used in the parallelized calculation.

[1] D. Sanwal, G. G. Pavlov, V. E. Zavlin, and A. A. Teter, Astrophys. J. **574**, L61 (2002).
[2] S. Mereghetti, A. de Luca, P. A. Caraveo, W. Becker, R. Mignami, and G. F. Bignami, Astrophys. J. **581**, 1280 (2002).
[3] F. Haberl, A. D. Schwope, V. Habaryan, G. Hasinger, and C. Motch, Astron. Astrophys. **403**, L19 (2003).
[4] F. Haberl, V. E. Zavlin, J. Trümper, and V. Burwitz, Astron. Astrophys. **419**, 1077 (2004).
[5] M. H. van Kerkwijk, D. L. Kaplan, D. L. Durant, S. R. Kulkarni, and F. Paerels, Astrophys. J. **608**, 432 (2004).
[6] K. Mori and C. J. Hailey, Astrophys. J. **564**, 914 (2002).
[7] K. Mori, J. C. Chonko, and C. J. Hailey, Astrophys. J. **631**, 1082 (2005).
[8] K. Mori and C. J. Hailey, Astrophys. J. **648**, 1139 (2006).
[9] S. Bücheler, D. Engel, J. Main, and G. Wunner, Phys. Rev. A. **76**, 032501 (2007).
[10] H. Ruder, G. Wunner, H. Herold, and F. Geyer, *Atoms in strong magnetic fields* (Springer, Heidelberg, 1994).
[11] I. Mayer, *Simple Theorems, Proofs, and Derivations in Quantum Chemistry* (Kluwer Academic/Plenum Publishers, New York, 2003).
[12] C. C. J. Roothaan, Rev. Mod. Phys. **23**, 69 (1951).
[13] L. I. Schiff and H. Snyder, Phys. Rev. **55**, 59 (1937).
[14] D. Neuhauser, K. Langanke, and S. E. Koonin, Phys. Rev. A **33**, 2084 (1986).
[15] M. C. Miller and D. Neuhauser, Mon. Not. R. Astro. Soc. **253**, 107 (1991).
[16] M. Rajagopal, R. W. Romani, and M. C. Miller, Astrophys. J. **479**, 347 (1997).
[17] D. Engel, M. Klews, and G. Wunner (2008), submitted to Comp. Phys. Comm.
[18] C. de Boor, SIAM J. Numer. Anal. **14**, 441 (1977).
[19] C. de Boor, *A practical guide to splines* (Springer, Heidelberg, 1978).
[20] V. S. Melezhik, Phys. Lett. A **230**, 203 (1997).

[21] V. S. Melezhik and D. Baye, Phys. Rev. C **59**, 3232 (1999).
[22] P. Capel, D. Baye, and V. S. Melezhik, Phys. Rev. C **68**, 014612 (2003).
[23] V. Canuto and D. C. Kelly, Astrophys. Space Sci. **17**, 277 (1972).
[24] W. Brent, *Algorithms for Minimisation Without Derivatives* (Prentice Hall, New Jersey, 1972).
[25] S. Zhang and J. Jin, *Computation of Special Functions* (Wiley-Interscience, New Jersey, 1996).
[26] M. V. Ivanov and P. Schmelcher, Phys. Rev. A **61**, 022505 (2000).
[27] P. Pröschel, W. Rösner, G. Wunner, H. Ruder, and H. Herold, J. Phys. B: At.Mol. Phys. **15**, 1959 (1982).